Journal of Alloys and Compounds 495 (2010) 663–666

Contents lists available at ScienceDirect

Journal of Alloys and Compounds

journal homepage: www.elsevier.com/locate/jallcom

A new pseudo-binary $Mg_6Ni_{0.5}Pd_{0.5}$ intermetallic compound stabilised by Pd for hydrogen storage

J.F. Fernández [a,*], F. Cuevas [b], F. Leardini [a], J. Bodega [a], J.R. Ares [a], G. Garcés [c], P. Pérez [c], C. Sánchez [a]

[a] Dpto. Física de Materiales, Facultad de Ciencias, Universidad Autónoma de Madrid, 28049 Madrid, Spain
[b] CMTR/ICMPE/CNRS, 2-8 rue Henri Dunant, 94320 THIAIS Cedex, France
[c] Centro Nacional de Investigaciones Metalúrgicas, CSIC, Av. Gregorio del Amo 8, 28040 Madrid, Spain

ARTICLE INFO

Article history:
Received 6 February 2009
Received in revised form 9 October 2009
Accepted 13 October 2009
Available online 22 October 2009

Keywords:
Hydrogen absorbing materials
Intermetallics
Crystal structure
Scanning Electron Microscopy SEM
X-ray Diffraction

ABSTRACT

The structural properties and chemical composition of a new pseudo-binary intermetallic compound $Mg_{6.01}Ni_{0.43}Pd_{0.53}$ stabilised by Pd have been studied by X-ray Powder Diffraction and Scanning Electron Microscope coupled to Energy Dispersive X-ray analysis. The intermetallic compound is isomorphous to Mg_6Pd (Cubic system, *F*-43*m* space group) with a lattice parameter of 20.1373 Å. The Mg atoms occupy the same atomic position than in Mg_6Pd while the Ni and Pd atoms share the 16*e* sites. The solubility limit of Ni in Mg_6Pd extents, at least, up to 11 wt%. The compound is stable up to melting which takes place at 800 K.

© 2009 Elsevier B.V. All rights reserved.

1. Introduction

Hydrogen storage for mobile applications is a major challenge for metal hydrides (MH). At present the inherent safety, high volumetric density and reversibility at moderate temperature and H_2-pressure conditions of MH are restricted to intermetallic AB_5, AB_2, and AB families in which A is an early transition metal or rare earth and B is a late transition metal. The mass capacity of these compounds is lower than 2 wt%. Looking for low weight metals is must for this type of applications. Magnesium hydride has a very high gravimetric density, 7.6 wt %, a low price and it is abundant on earth. However, high stability and slow kinetics preclude its direct use in mobile applications. Because of that, a lot of work has been developed in the past to overcome the kinetics [1,2] and thermodynamic [3–6] limitations. More recently, interest of theoreticians for MH [7–9] has brought new impulse to the quest for new destabilised magnesium alloys. In most cases the results from such work point to metastable phases as possible candidates for destabilised magnesium hydride alloys.

There have been some reports regarding hydrogenation properties of metastable Mg_6Ni compounds [10,11]. Alloying of Mg and Ni with Mg_6Ni stoichiometry by conventional metallurgical methods, i.e. at thermodynamic equilibrium, results in a two phase $Mg + Mg_2Ni$ material [12]. By melt spinning an amorphous alloy is obtained, which crystallises isomorphous to the Mg_6Pd intermetallic alloy [13] at 573 K [14]. This metastable alloy transforms to the $Mg + Mg_2Ni$ two phase alloy at a higher temperature (~673 K). The hydrogenation properties of the metastable Mg_6Ni phase have been studied at room temperature by electrochemical methods [11]. However, full characterisation of the hydrogen interaction with this compound has not been obtained due to its metastable character.

In this paper we show that it is possible to stabilise the Mg_6Ni compound by partial substitution of Ni by Pd. The intermetallic compound $Mg_6Pd_{0.5}Ni_{0.5}$ crystallises in the same space group as Mg_6Pd. A previous assessment of the ternary Mg–Ni–Pd phase diagram reports that Ni solubility in the Mg_6Pd phase only extends up to ~3 wt% at 673 K [15]. Our results demonstrate that the Ni solubility limit extends, at least, up to 11 wt%.

2. Experimental

An alloy with nominal composition $Mg_6Ni_{0.5}Pd_{0.5}$ was prepared by induction melting under argon followed by casting. The initial constituents were a two phase alloy $Mg + Mg_2Ni$ (47.5 wt%:52.5 wt%) and elemental Mg and Pd. The alloy was brittle having a metallic appearance. The samples were subjected to two different thermal annealing treatments: 657 K in vacuum for three days and 698 K in Ar for five days. Cooling was achieved by removing the sample from the furnace. In the following these samples will be labelled as A657 and A698, respectively. Chemical composition was studied by means of Scanning Electron Microscopy coupled to Energy Dispersive X-ray Analysis (SEM-EDX) on a HITACHI S-3000N OK at 20 keV. Specimens for SEM-EDX analysis were embedded in epoxy resin and polished with diamond paste and colloidal silica down to 0.25 μm. Structural characterisation was obtained by X-ray Powder Diffraction (XRPD) on a X'Pert Pro Panalitical θ–2θ diffractometer (fil-

---

* Corresponding author. Tel.: +34 914976704; fax: +34 914978579.
E-mail address: josefrancisco.fernandez@uam.es (J.F. Fernández).

0925-8388/$ – see front matter © 2009 Elsevier B.V. All rights reserved.
doi:10.1016/j.jallcom.2009.10.090

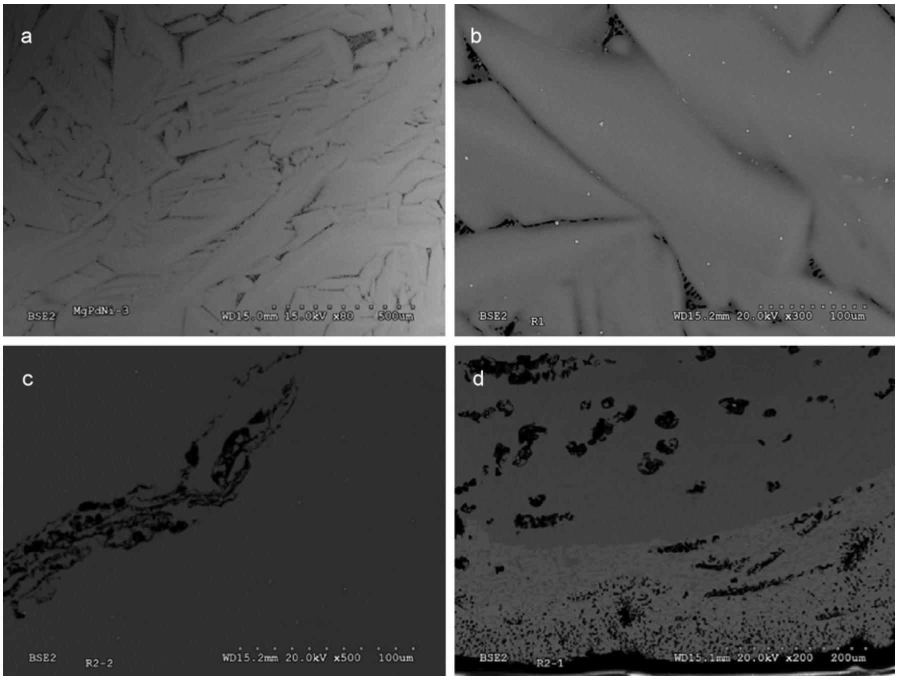

Fig. 1. BSE images for A657 (a and b) and A698 (c and d) samples. Bright spots on (b) are due to colloidal silica used for the polishing. The black features of (c) are voids induced by polishing.

tered Cu-K$_\alpha$, Bragg–Brentano geometry, 2θ range 10–90°, step size 0.012°, counting time 2.7 s). The diffraction patterns were analysed using the Rietveld method with the Fullprof software [16]. Bulk density was measured with a Helium Pycnometer (Micromeritics Accupyc 1330). The thermal stability of the alloy was studied by Differential Scanning Calorimetry (DSC) in a PerkinElmer DSC-4 calorimeter at a heating rate of 20 K/min under argon atmosphere.

3. Results

Fig. 1 shows Backscattered Electron (BSE) images of polished samples after annealing at 657 K (Fig. 1a and b) and 698 K (Fig. 1c and d). In Fig. 1a and b we can observe that the A657 sample is chemically homogeneous with a minor amount of black precipitates along the grain boundaries (Fig. 1b). The precipitates mainly consist of magnesium as revealed by EDX analysis. On the other hand, for the A698 sample no Mg precipitates are found (Fig. 1c). The black features observed in Fig. 1c are voids induced by polishing. Quantitative chemical composition was obtained from EDX line scan analysis. The results are presented in Fig. 2a (A657) and Fig. 2b (A698). The Mg composition is homogenous for both samples. A clear anti-correlation between the Ni and Pd composition can be noted for A657. The homogeneity of Ni and Pd composition clearly improves with the annealing treatment at 698 K. The average composition is $Mg_{6.00(4)}Ni_{0.39(5)}Pd_{0.63(5)}$ for A657 and $Mg_{6.01(4)}Ni_{0.43(3)}Pd_{0.53(3)}$ for A698. Both samples are poorer in Ni and richer in Pd as compared to the nominal alloy composition. It should be mentioned that, although in a very small amount, we have observed some segregation of Pd and Ni at the surface of the A698 sample (Fig. 1d). This is probably connected to the exponential increase in Mg vapour pressure which starts to be important at the temperature of that annealing ($P_{vap} \sim 1$ Pa). This segregation seems to indicate that a reduction of Mg content leads to a phase separation of the alloy into several other phases, like Mg_2Ni or Mg_6Pd.

XRPD pattern of the A657 sample is presented in Fig. 3. All diffraction peaks can be indexed in the *F*-43*m* space group with a lattice parameter of 20.1373(3) Å. It is larger than that of Mg_6Pd, $a = 20.1080$ Å. The Rietveld refinement has been done by assuming that the Mg atoms occupy the same atomic positions than in Mg_6Pd compound while the Ni and Pd atoms share the 16*e* positions. No additional peaks were observed. The low amount of Mg precipitates seen in Fig. 1a is below the detection limit of XRPD measurements. Similar results were obtained for the A698 sample,

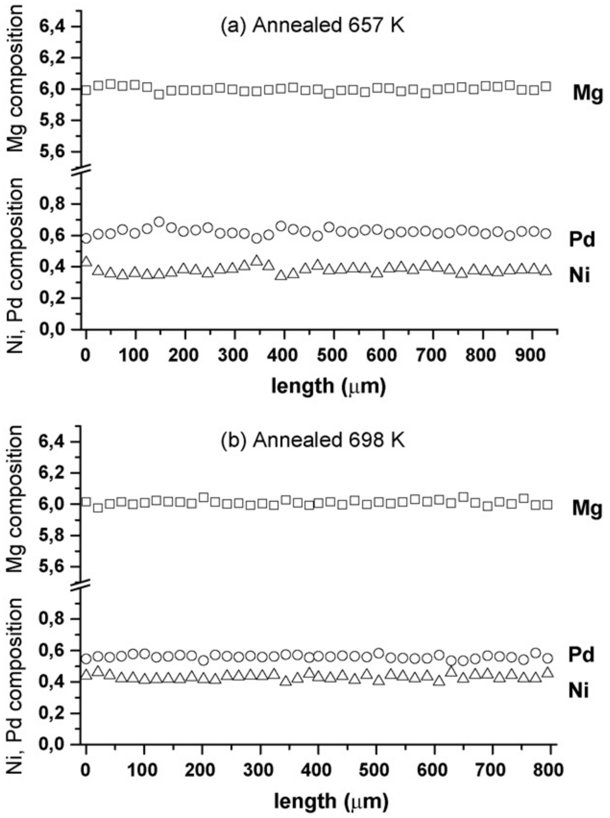

Fig. 2. Mg–Ni–Pd chemical composition for the A657 (a) and A698 (b) samples as measured from line scan EDX analysis.

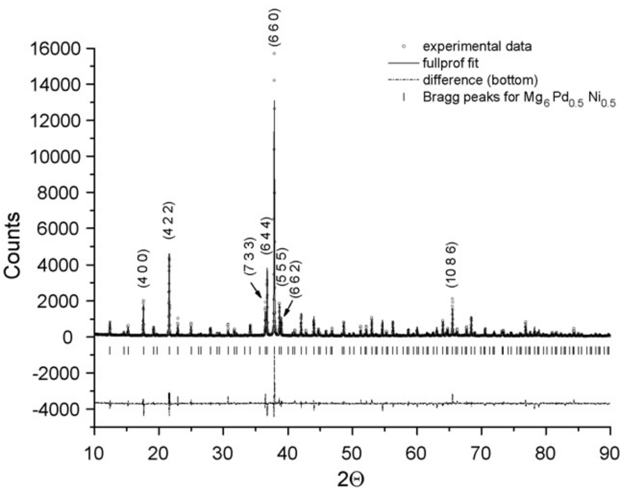

Fig. 3. XRPD pattern for the A657 sample (circles) together with the Rietveld refinement obtained with the Fullprof software (solid line). Bragg peaks for the $Mg_6Ni_{0.5}Pd_{0.5}$ phase are shown as vertical bars. Difference between the calculated and the experimental patterns is shown at the bottom of the graph (dashed line). Miller indices are given for the main peaks in the pattern.

being the only difference a slight decrease in the lattice parameter 20.1333(5) Å. The agreement factors for the fitting were $R_p = 16.0$, $R_{wp} = 20.6$, $R_{Bragg} = 15.5$ and $\chi^2 = 6.53$.

The thermal stability of the new phase was studied by thermal analysis. Fig. 4 shows DSC heating and cooling runs for the A657 sample. No thermal events were observed during heating until 800 K. At this temperature an endothermic peak is measured. On cooling, a more complicated exothermic event is observed. Most probably DSC peaks are related to the melting (on heating) and solidification (on cooling) of the alloy that happen at temperatures of 800 K and 762 K, respectively. Subsequent heating and cooling runs of the sample show essentially the same DSC curves. The heat of melting is $(1/7)\Delta H_m = 7.2$ kJ/mol while the entropy of melting is $(1/7)\Delta S_m = 9.0$ J/K mol. A slightly larger value is measured for the heat of solidification on cooling ($(1/7)\Delta H_m = 7.7$ kJ/mol). The observed values of heat and entropy are in favour of the thermal events as being due to the melting of the alloy. For comparison, the heat of melting of Mg_2Cu is two times larger, $(1/3)\Delta H_m = 13.7$ kJ/mol [17].

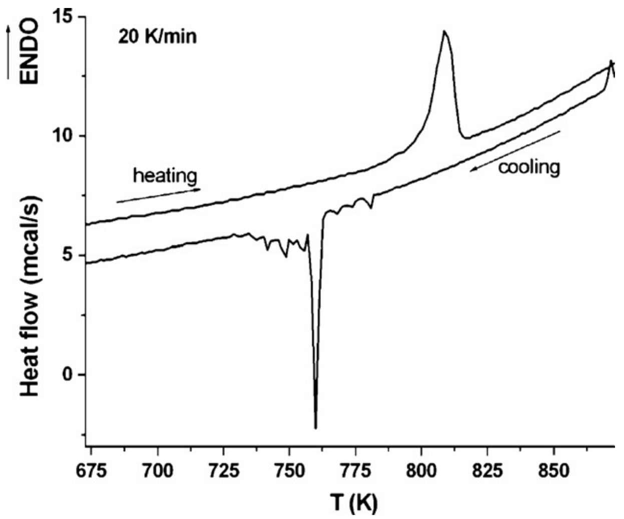

Fig. 4. DSC scans for heating and cooling of the A657 sample. The curves were obtained under Ar at a heating/cooling rate of 20 K/min.

4. Discussion

The main question we would like to answer is the following: the new phase we have found is it a stable or a metastable phase? Recently, an assessment of the ternary phase diagram of the Mg–Ni–Pd system has been published [15]. According to that work, at 673 K a three-phase field composed of $\rho(Mg_6Pd)$, $\beta(Mg_2Ni)$ and $\varepsilon(Mg)$ phases is formed at the Mg-rich corner of the phase diagram. At this temperature, the limit of solubility of Ni in the ρ phase does not extent more than 3 wt% Ni. In addition, several eutectic reactions in the Mg-rich corner of the Mg–Ni–Pd phase diagram have been reported: a four-phase eutectic type ($L \rightarrow \varepsilon + \beta + \rho$, 763 K), a eutectic pseudo-binary ($L \rightarrow \beta + \rho$, 808 K), and two eutectic binary ($L \rightarrow \varepsilon + \beta$, 780 K and $L \rightarrow \varepsilon + \rho$, 813 K) reactions. According to that work, our single-phase samples should correspond to a metastable phase. However, it is difficult to understand how the sample A698 can be metastable. This sample with composition 64 wt% Mg, 11 wt% Ni, 25 wt% Pd ($Mg_{6.01(4)}Ni_{0.43(3)}Pd_{0.53(3)}$) has been annealed for 5 days at 698 K. After this long thermal treatment the SEM-EDX and XRPD studies clearly indicate that the sample is a homogeneous pseudo-binary single-phase alloy isomorphous to the ρ phase. In addition, DSC calorimetric measurements show that no thermal events are observed when the alloy is heated up to the melting point. Therefore, we conclude that the phase we have found is stable and that the solubility limit of Ni in the ρ phase should extent, at least, up to 11 wt%.

A possible explanation for the discrepancy between our results and the published phase diagram can lay on the small amount of segregated Ni and Pd rich phases we have found at the surface of the A698 sample. As we have only observed such effect at the surface of the sample, we have concluded that it should be driven by the loss of Mg due to evaporation. Therefore, it could be possible that for the experiments quoted in reference [15], this effect is responsible for a misleading assignment of the equilibrium phases.

It is interesting to note that the melting of the alloy takes place at 800 K, a temperature similar to that quoted in [15] for the eutectic pseudo-binary ($L \rightarrow \beta + \rho$ (808 K)) and not far away from the other eutectic temperatures. On the other hand, the melting point of the intermetallic Mg_6Pd takes place at a much higher temperature (above 973 K). It seems that the thermal behaviour of the Ni-substituted alloy close to the melting temperature resembles more that of the two phase system ($\beta + \rho$) than that of the single-phase intermetallic compound. Therefore, we cannot rule out that at temperatures very close to the melting point, the sample can decompose to the $\beta + \rho$ phases. This decomposition should be kinetically hindered as we do not observe any thermal event in the DSC measurements until melting.

The lattice parameter of the new phase, 20.1373(3) Å is considerably larger than those of Mg_6Pd (20.108(2) Å [13]) and the metastable Mg_6Ni (20.09 Å [14] or 19.987(1) Å [11]). As a larger atom like Pd (atomic radius $r_{Pd} = 1.37$ Å) is substituted by a smaller one like Ni ($r_{Ni} = 1.25$ Å) the lattice parameter should have increased with the Pd for Ni substitution. However, this discrepancy is not so relevant if we consider the low amount of substituted Pd atoms (one out of fourteen atoms) and the existence of a homogeneity region for the Mg_6Pd phase. In the binary Mg–Pd system, this phase occurs from 85 at% Mg to 87.2 at% Mg, being the homogeneity range probably accommodated by partial substitution of Pd by Mg in the 16*e* site (atom no.12) and, also, by partial occupancy of Mg atoms in the 4*d* site [13]. Since the atomic radius of Mg ($r_{Mg} = 1.60$ Å) is much larger that those of Pd and Ni, the lattice parameter is expected to depend much strongly on the Mg content than on the Ni for Pd substitution. Small variations on the phase stoichiometry would hide the changes of the lattice parameters induced by the Ni for Pd substitution. More information about crystallography and other properties of the new phase have been published recently [18,19].

The bulk density has been calculated from the atomic composition obtained from EDX analysis and the volume of the unit cell, 8165.9(3) Å^3. To estimate the bulk density we assume full occupancy of all sites in the cubic structure, rending a total amount of 396 atoms in the unit cell. From this value, the cell volume and the atomic composition measured by EDX we have arrived to a calculated density of 2.62(2) g/cm^3, in fairly good agreement with the bulk density measured with the helium pycnometer, 2.58(1) g/cm^3.

The fitting of the XRPD pattern can be considered good though some discrepancies between the calculated and experimental intensities for some of the peaks are apparent from the difference plot. This is a clear indication that a better refinement of the Pd and Ni occupancy factors is needed. It should be taken into account that the high difference in electronic density between Ni and Pd and the high number of atoms in the unit cell (∼396) make the XRPD spectra very sensitive to the Ni to Pd substitution. In particular, the 16*e* site (atom no.12 in ref. [13]) in the structure cannot be refined just from the XRPD data as the three elements, Mg, Pd or Ni, can occupy such site. Neutron diffraction (ND) measurements are underway in order to determine the occupation factors for all atoms by a simultaneous refinement of ND and XRPD data.

5. Conclusions

A new pseudo-binary $Mg_6Ni_{0.5}Pd_{0.5}$ intermetallic alloy stabilised by Pd has been found. The alloy is isomorphous to Mg_6Pd and it crystallise in the cubic system, in the space group *F*-43*m*. The lattice parameter is $a = 20.1373(3)$ Å, slightly larger than the value for Mg_6Pd. The Mg atoms occupy the same atomic position as that in the parent alloy Mg_6Pd while the Ni and Pd atoms share the 16e positions in the cubic structure. The atomic composition of the alloy as measured by EDX is $Mg_{6.00(4)}Ni_{0.39(5)}Pd_{0.63(5)}$ for the sample annealed at 657 K and $Mg_{6.01(4)}Ni_{0.43(3)}Pd_{0.53(3)}$ for that annealed at 698 K. The density of the compound is 2.58(1) g/cm^3 in good agreement with the calculated one from the EDX composition and the cell volume, 2.62(2) gr/cm^3. Our results demonstrate that the solubility limit of Ni in the Mg_6Pd phase extent, at least, up to 11 wt%. The alloy melts at 800 K, a temperature close to the eutectic pseudo-binary reaction ($L \rightarrow \beta + \rho$, 808 K).

Acknowledgements

The authors thank the Spanish Ministry of Education and Science, MEC, for financial support under contract N° MAT2008-06547-C02-01. We thank F. Moreno for technical assistance.

References

[1] J. Huot, G. Liang, R. Schultz, Appl. Phys. A 72 (2001) 187.
[2] B. Sakintuna, F. Lamari-Darkrim, M. Hirscher, Int. J. Hydrogen Energy 32 (2007) 1121–1140.
[3] J.J. Reilly, R.H. Wiswall, Inorgan. Chem. 7 (1968) 2254.
[4] J.J. Reilly, R.H. Wiswall, Inorgan. Chem. 6 (1967) 2220.
[5] J. Didisheim, P. Zolliker, K. Yvon, P. Fisher, J. Schefer, M. Gubelmann, A.F. Williams, Inorgan. Chem. 23 (1984) 1953.
[6] P. Zolliker, K. Yvon, P. Fisher, J. Schefer, Inorgan. Chem. 24 (1985) 4177.
[7] Y. Takahashi, H. Yukawa, M. Morinaga, J. Alloys Compd. 242 (1996) 98–107.
[8] Y. Song, Z.X. Guo, R. Yang, Phys. Rev. B 69 (2004) 094205.
[9] C.P. Broedersz, R. Gremaud, B. Dam, R. Griessen, O.M. Lovvick, Phys. Rev. B 77 (2008) 024204.
[10] A. Teresiak, M. Uhlemann, J. Thomas, A. Gebert, J. Alloys Compd. 475 (2009) 191–197.
[11] T. Spassov, U. Koster, J. Alloys Compd. 287 (1999) 243–250.
[12] G.M. Friedelmeier, J.C. Bolcich, Int. J. Hydrogen Energy 13 (8) (1988) 467–474.
[13] S. Samson, Acta Cryst. B 28 (1972) 936.
[14] A.T.W. Kempen, H. Nitsche, F. Sommer, E.J. Mittemeijer, Metallurg. Mater. Trans. A 33A (2002) 1041–1050.
[15] K.P. Gupta, J. Phase Equilibria Diffus. 25 (2) (2004) 191–194.
[16] J. Rodriguez Carvajal, Phys. B 192 (1993) 55.
[17] H. Feufel, F. Sommer, J. Alloys Compd. 224 (1995) 42–54.
[18] F. Cuevas, J.F. Fernández, J.R. Ares, Leardini Leardini, M. Latroche, J. Solid State Chem. 182 (2009) 2890–2896.
[19] J.F. Fernández, J.R. Ares, F. Cuevas, J. Bodega, F. Leardini, C. Sánchez, Intermetallics 18 (2010) 233–241.